Observations of cavity polaritons in one-dimensional photonic crystals containing a liquid-crystalline semiconductor based on perylene bisimide units

T. Sakata, M. Suzuki, T. Yamamoto, S. Nakanishi, M. Funahashi, and N. Tsurumachi

Faculty of Engineering, Kagawa University, 2217-20 Hayashi-cho, Takamatsu 761-0396, Japan

We investigated the optical transmission properties of one-dimensional photonic crystal (1D-PC) microcavity structures containing the liquid-crystalline (LC) perylene tetracarboxylic bisimide (PTCBI) derivative. We fabricated the microcavity structures for this study by two different methods and observed the cavity polaritons successfully in both samples. For one sample, since the PTCBI molecules were aligned in the cavity layer of the 1D-PC by utilizing a friction transfer method, vacuum Rabi splitting energy was strongly dependent on the polarization of the incident light produced by the peculiar optical features of the LC organic semiconductor. For the other sample, we did not utilize the friction transfer method and did not observe such polarization dependence. However, we did observe a relatively large Rabi splitting energy of 187 meV, probably due to the improvement of optical confinement effect.

I. INTRODUCTION

The interaction between light and condensed matter in a microcavity in the strong coupling regime has long been extensively studied. In this regime, mixing between the photon modes and the electronic states of matter, such as the exciton, produces cavity polaritons [1]. In such systems, various phenomena such as Bose-Einstein condensation [2], low-threshold polariton lasing [3], and ultrafast optical-parametric amplification [4] have been reported. Thus far, cavity polaritons have been observed in various kinds of materials such as semiconductor quantum wells [5], quantum dots [6], inorganic crystal [7], and organic material [8].

Especially, cavity polaritons in organic materials have been attracting attention because they display a large Rabi splitting energy even at room temperature. Although it has been considered difficult to observe cavity polaritons using organic materials because of their large inhomogeneous broadening, cavity polaritons has in fact been reported in several organic materials—such as cyanine J aggregates [9–11], polymers [12], and single crystals [13] owing to their large oscillator strengths and exciton binding energies. In addition, giant Rabi splitting that even reaches the ultrastrong coupling regime has been observed recently [14,15]. Although the magnitude of Rabi splitting is not simple as it is determined by factors such as the oscillator strength of the materials and the mode volume of the cavity, such large Rabi splitting is more likely to be observed in an ordered molecular system such as a single crystal because of the large oscillator strength, than in an amorphous system.

Device applications require high-quality and uniform film that can be produced by inexpensive and simple fabrication methods. In spite of the high electrical conductivities of organic single-crystal systems, problems with fabrication costs and process complexity have remained. In order to solve these problems, it is proposed to utilize a liquid crystalline (LC) material [16]. LC materials have the advantage that formation of high-quality films in which molecules are regularly ordered is possible even by an inexpensive and simple solution processes such as amorphous. Recently, a LC organic semiconductor has been reported that exhibits a carrier mobility almost as high as that of an organic crystal, and rapid future progress is expected [17–19]. Furthermore, for optical applications, various types of LC organic semiconductors such as triphenylene derivatives [20], phthalocyanine derivatives [21], oligothiophene derivatives [22], and perylene derivatives [23] were investigated. These materials are expected to have high oscillator strengths because of their high degree of molecular ordering. This is advantageous for cavity-polariton observations. There is also expectation that delocalized Frenkel excitons in LC organic semiconductor exhibit coherent characteristics.

In this paper, we report the successful observation of cavity polaritons using LC organic semiconductors. For this work, we utilized a perylene tetracarboxylic bisimide (PTCBI) derivative, which has also been reported to have high electron mobilities [24,25]. We find that large polarization anisotropy peculiar to LC organic semiconductors affects the Rabi splitting energy in the cavity polaritons. We also report the possibility of larger Rabi splitting, which depends upon the method of fabrication of the microcavity structure.

II. EXPERIMENTAL PROCEDURE

For our cavity polaritons studies, we synthesized LC PTCBI bearing four 1,1,1,3,3-pentamethyldisiloxane chains. The chemical synthesis scheme and other basic properties of this material have previously been described in the literature [25]. The chemical structure of this sample is shown in Fig. 1(a). In order to align the LC PTCBI derivative uniaxially, we performed a rubbing treatment on the substrate by a friction transfer method in this study. Teflon block was pressed on a heated substrate using a hot-stage, and a nanometer scale groove was formed on the substrate by moving the block in one direction [26]. After this treatment, a chloroform solution of PTCBI derivative was dropped on the substrate and its thin film was formed by spin coating. At room temperature, this sample shows a rectangular columnar LC phase. We already confirmed that the rubbing direction and the lamination direction of the columnar layer were parallel as shown in Fig. 1(b) [25]. Polarizing optical micrographs of uniaxially ordered LC PTCBI derivative on the substrate performed to
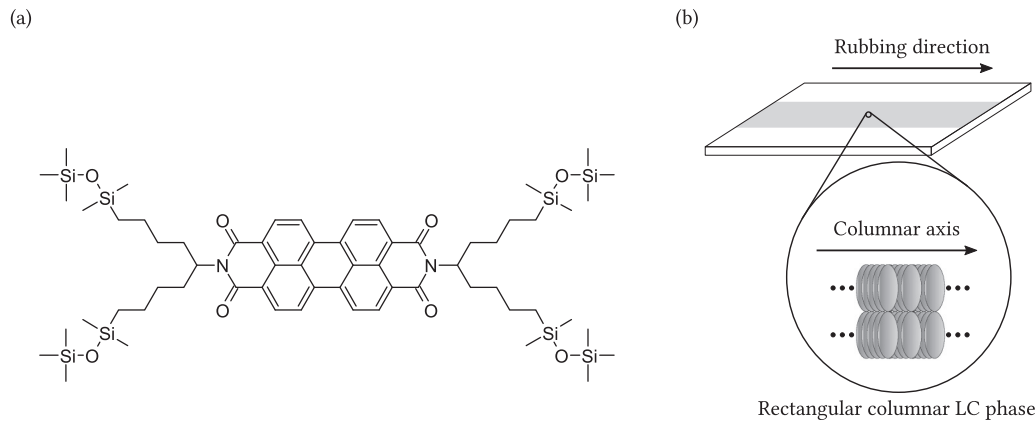
(a)

(b)

FIG. 1. (a) Chemical structure of PTCBI with four 1,1,1,3,3-pentamethyldisiloxane chains. (b) Relationship between the rubbing direction and the lamination direction of the columnar layer.

the rubbing treatment was shown in Fig. 2. Since this sample was well aligned with a large area of several hundred μm order, one can see that the color of the entire image greatly changed owing to the birefringence of the liquid crystal.

For the present investigations, we fabricated microcavity-type one-dimensional photonic crystal (1D-PC) samples with LC PTCBI thin film by two different ways. In both cases, the LC PTCBI film was sandwiched between two dielectric mirrors, each having a structure comprising quarter-wave stacks of SiO_2 and TiO_2. The center wavelength of each mirror was 600 nm. The range of the stop band of the 1D-PC dielectric mirrors used in this study corresponded to energy from 1.64 eV–2.40 eV. In the first sample (cavity A), we formed nanoscale grooves on one of the dielectric mirror surfaces by the friction transfer method described above and we formed the PTCBI thin film by spin coating on the treated mirror. Then the other mirror was placed on the PTCBI surface and fixed to fabricate the 1D-PC microcavity. Here, the period of quarter-wave stacks was five. The thickness of the cavity layer was gradually and intentionally changed from the edge of the sample by applying mechanical pressure to the glass substrates on both sides of the 1D-PC before the solvent had completely evaporated. The cavity layer is therefore wedge shaped, and the cavity resonance shifts as the position of the incident light

beam is moved along the wedge [11,27]. In the second sample (cavity B), we placed two uncoated mirrors face-to-face and fixed them in a position after adjusting the spacing to a wedge shape. Here, the period of quarter-wave stacks was six. The reflectance of the mirrors was higher than that of sample A. We then injected a chloroform solution of the PTCBI derivative into the spacing between the two mirrors and left it to dry for several days [28,29].

We investigated the absorption properties of both the chloroform solution of PTCBI and the LC PTCBI film. Especially, in case of the LC PTCBI film, the polarization dependence of absorption spectra was measured to investigate alignment direction. We defined the polarization angle to be 0° parallel to the rubbing direction, and we changed it in ten-degree increments up to 90°. We also investigated the dependence of the transmission spectra of the 1D-PC microcavities on the position of the light beam along the wedge-shaped cavities—which we term the incident position—to obtain the polariton dispersion curve. For the 1D-PC microcavity, the cavity mode shifts with changing the incident position. In addition, we measured the polarization dependence of the transmission spectra.

III. RESULTS AND DISCUSSION

The absorption spectra of the chloroform solution of the PTCBI derivative (1×10^{-5} M) and of the LC PTCBI film at room temperature are shown in Fig. 3, as dashed and solid lines, respectively. For the low-concentrated chloroform solution of the PTCBI derivative, we observed strong absorption by the S_0-S_1 transition at 2.38 eV, together with the well-resolved vibronic structure peculiar to the monomeric perylene bisimide moiety [30]. In contrast, for the LC PTCBI film, although the spectra width become broader due to the electronic coupling, we observed an absorption band composed of multiple absorption peaks at almost the same energy band as for the monomer in solution. Moreover, we observed a new absorption peak at 2.26 eV on the low-energy side of the absorption spectrum. Würthner's group has reported that a similar absorption peak appeared in the low-energy side by forming a LC columnar phase, which was originated from the self-organized packing in the PTCBI derivative [30]. We
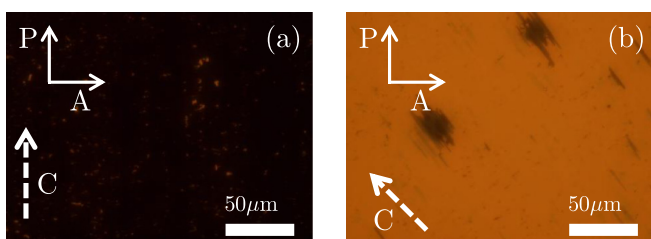

FIG. 2. Polarizing optical micrographs of uniaxially ordered LC PTCBI derivative on the substrate performed to the rubbing treatment. Here, P and A are optical axis direction of polarizer and analyzer. Dashed arrow C indicated the columnar axis direction. Since this sample was well aligned with large area of several hundred microns order, one can see that the color of entire image greatly changed owing to the birefringence of the liquid crystal when the angle of C with respect to P was changed from (a) 0° to (b) 45°.
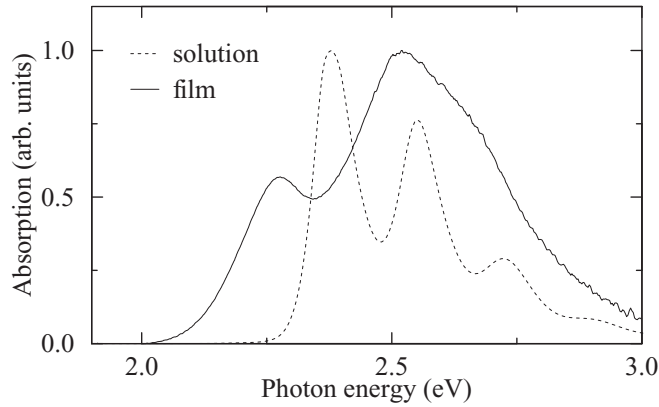
FIG. 3. Absorption spectra of the chloroform solution of the PTCBI derivative (dashed line) and the LC PTCBI film (solid line) at room temperature.

regard the low-energy peak observed in this study to have the same origin.

The polarization dependence of the absorption spectra of the LC PTCBI film at room temperature is shown in Fig. 4. We observed clear dichroism, with the absorption at minimum when the polarization angle of the incident light is $0°$ and at maximum when it is $90°$. At 2.26 eV, the ratio of the absorbance for polarization angle of $90°$–$0°$ was 3.3:1. At the 90-degree polarization angle, the electric field direction of the light was perpendicular to the rubbing direction, which is identical to the columnar axis. Because the direction of the transition dipole moment of the PTCBI molecule is parallel to the molecular plane, the absorption is larger at this angle. These experimental results suggest that the PTCBI molecules are well oriented on the rubbed substrate.

We next investigated the transmission properties of the 1D-PC containing the LC PTCBI film (cavity A). The incident-position dependence of the transmission spectra of this sample at room temperature is shown in Fig. 5. We set the polarization angle to $90°$ for this measurement because the absorption of the PTCBI film is maximum at that angle. When the resonant energy of the cavity matches the transition energy of the PTCBI at 2.26 eV—accomplished by changing the incident
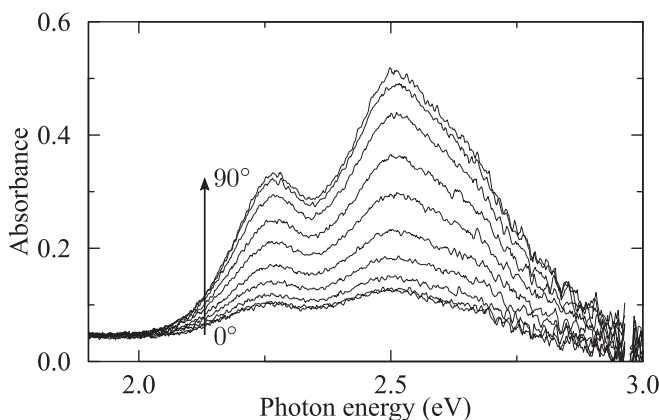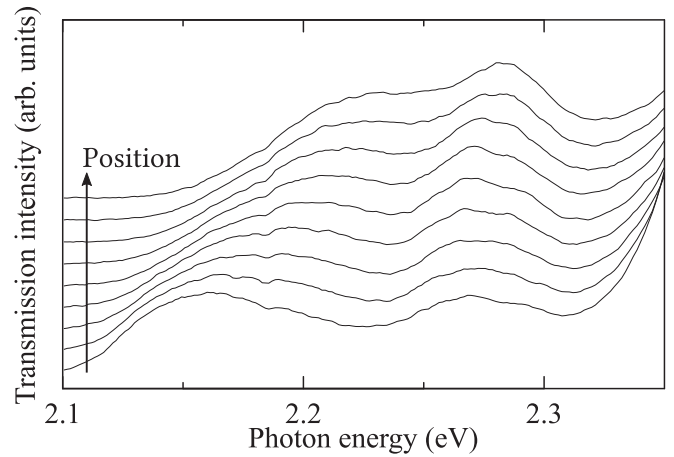

FIG. 5. Incident position dependence of the transmission spectra of cavity A at room temperature. Here, the polarization angle was set to $90°$.

position of the light—the transmission peak of the microcavity splits in two owing to the creation of cavity polaritons. In this sample, the light at 2.50 eV could not confined in the cavity, and did not strongly couple to the exciton transition on the higher-energy side because the stop band of the mirrors did not cover at the photon energy. We also measured the dependence upon the incident position of the transmission spectra of the same sample when the polarization angle was set to $0°$. Similar changes in the transmission spectra were observed. The incident-position dependence of the energy of the transmission peak corresponds to the dispersion curve of the cavity polariton, as can be observed in Fig. 6. The open and closed circles are the dispersion curves with the polarization angle set to $90°$ and $0°$, respectively. The solid and dashed lines are the fitting curves obtained using the following formula from the cavity polariton theory [31]:

$$E_{u,l}(x) = \frac{E_{ph}(x) + E_{ex}}{2} \pm \frac{1}{2}\sqrt{(E_{ph}(x) - E_{ex})^2 + \Delta E^2}. \quad (1)$$

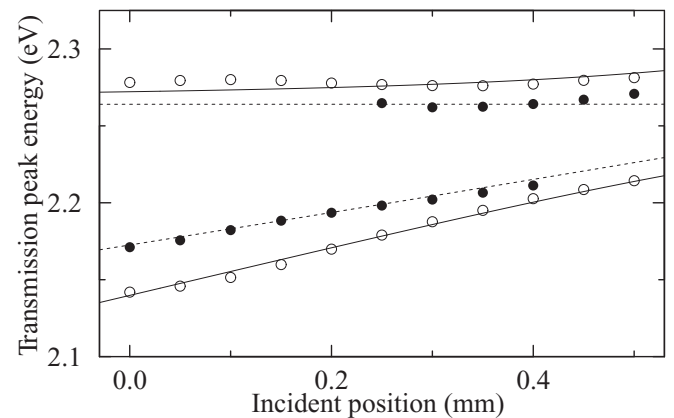FIG. 4. Polarization dependence of absorption spectra of the LC PTCBI film at room temperature.

FIG. 6. The incident-position dependence of the energy of the transmission peak of cavity A corresponds to the dispersion curve of the cavity polariton. The open and closed circles show the dispersion curves with the polarization angle set to $90°$ and $0°$, respectively. The solid and dashed lines are the fitting curves described in Eq. (1).
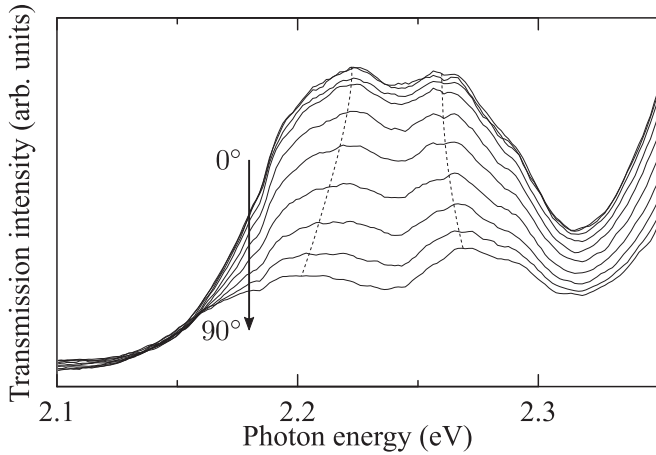
FIG. 7. Polarization dependence of the transmission spectra of cavity A at room temperature.

FIG. 8. Incident position dependence of the transmission spectra of cavity B at room temperature.

Here, $E_{\mathrm{u}}(x)$ and $E_{\mathrm{l}}(x)$ are the upper and lower polariton energies as functions of the incident position, respectively. The quantities $E_{\mathrm{ph}}(x)$, E_{ex}, and ΔE are, respectively, the energy of the cavity photon mode, the exciton transition energy, and the Rabi splitting energy. Here, we assumed that the thickness of the cavity layer changes linearly with the position with the inclination θ, the energy $E_{\mathrm{ph}}(x)$ of the cavity mode was expressed by the following equation:

$$E_{\mathrm{ph}}(x) = \frac{hc}{L_{\mathrm{cav}}(x)} = \frac{hc}{L_{\mathrm{cav}}(0) - x\tan(\theta)}. \tag{2}$$

In fact, it has been confirmed experimentally that this assumption is valid in a blank cavity. Here, $L_{\mathrm{cav}}(x)$ is the thickness at the position x and $x = 0$ was the position where measurement was started. In our fitting, θ and $L_{\mathrm{cav}}(0)$ were obtained as parameters in addition to Rabi splitting energy ΔE. By this fitting Eq. (1) to the data plotted in Fig. 6, we obtained Rabi splitting energies of 63.8 meV and 33.1 meV for polarization angles of 90° and 0°, respectively.

The polarization dependence of the transmission spectra of cavity A at room temperature is shown in Fig. 7. We fixed the incident position of the light at the location where the peak splitting was smallest. At all polarization angles, the splitting of the transmission peak occurs near 2.26 eV, which is the absorption peak of the LC PTCBI film. Changing the polarization angle from 0°–90° increases the absorption of the LC PTCBI film, causing the transmittance of the peaks to decrease and the amount of peak splitting to increase. The experimentally obtained ratio of the Rabi splitting at polarization angle 90° to that at 0° was 1.93:1. The vacuum Rabi splitting energy ΔE is represented by [32]

$$\Delta E = \sqrt{\frac{2N\mu^2\hbar\omega}{\epsilon V_0}}, \tag{3}$$

where N, ϵ, V_0, and μ are the number of oscillators interacting with the photon mode, the dielectric constant of the cavity layer, the mode volume of the microcavity, and the transition dipole moment, respectively. The transition dipole moment is
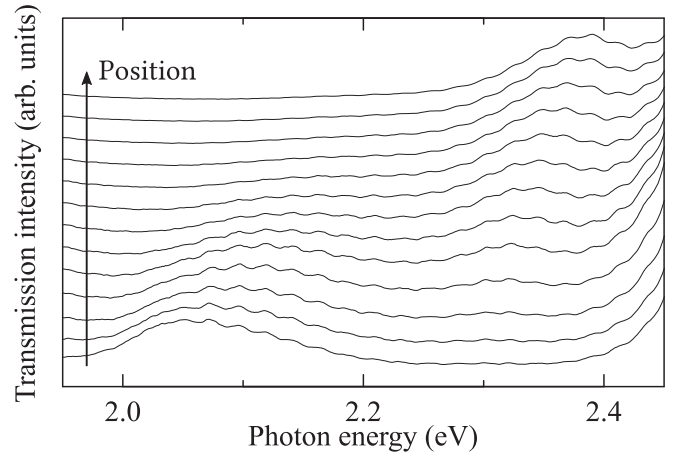
related to the absorption spectrum by

$$N\mu^2 \propto Nf \propto \int \alpha(\omega)d\omega, \tag{4}$$

where, f and $\alpha(\omega)$ are the oscillator strength and absorption coefficient, respectively. The vacuum Rabi splitting energy is thus proportional to the square root of the absorption coefficient. That is, the ratio of the oscillator strength in each polarization direction corresponds to the ratio of the absorbance, as shown in Fig. 4. Equation (3) gives the ratio of the Rabi splitting at polarization angle 90° to that at 0° to be 1.82 : 1, which is comparable to the experimentally obtained value of 1.93 : 1. This suggests that the Rabi splitting energy depends strongly on the polarization of the incident light produced by the optical properties of the LC organic semiconductors.

Next, we investigated the transmission properties of the 1D-PC based on the LC PTCBI film consisting of randomly oriented domains (cavity B). The dependence of the transmission spectrum at room temperature upon the incident position of the light is shown in Fig. 8. Here, the incident light was unpolarized, and we observed typical cavity polariton doublet behavior. Figure 9 shows that the incident-position dependence of the transmission peak energy of cavity B corresponds to the dispersion curve of the cavity polariton. From this result, the Rabi splitting energy was estimated to be 187 meV, a considerably larger value than that obtained for cavity A. There may be several reasons for this difference. Since the rubbing treatment was not performed for cavity B, the roughness of the mirror surface may have been suppressed, improving the confinement of the light as compared to cavity A. In addition, factors such as the difference in mirror reflectance, cavity length, or in the number of molecules coupled with cavity photons might affect the results. In this sample, the transmission spectra were almost the same at all polarization angles. Since no orientation treatment was performed on this sample, the domain size of the LC PTCBI appears to be smaller than the spot size of the incident light, so that the transmission spectra are averaged over a number of domains. In this sample, although we did not observe any polarization dependence peculiar to the LC organic semiconductor, we
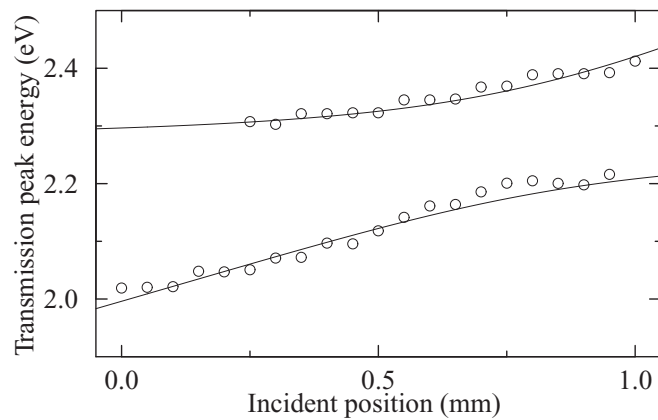
FIG. 9. The Incident position dependence of the energy of the transmission peak of cavity B corresponds to the dispersion curve of the cavity polariton. The open circles are the dispersion curves and the solid lines are the fitting curves.

found the LC PTCBI derivative to be an interesting material that can have a relatively large Rabi splitting energy. Since the magnitude of the Rabi splitting energy depends sensitively on the mode volume, larger Rabi splitting can be expected for a

Fabry-Pérot microcavity fabricated with metal mirrors rather than with 1D-PC type dielectric multilayer mirrors [33,34].

IV. CONCLUSION

In summary, we fabricated 1D-PC structures containing LC PTCBI-derivative thin films using two different methods. In both samples, we have successfully observed cavity polaritons by means of transmission measurements. For one sample (cavity A), the Rabi splitting energy was strongly dependent on the polarization of the incident light produced by the optical properties of the LC organic semiconductors. In the other sample (cavity B), although we did not observe any polarization dependence peculiar to the LC organic semiconductor, we did find a relatively large Rabi splitting energy of 187 meV.

[1] A. V. Kavokin, J. J. Baumberg, G. Malpuech, and F. P. Laussy, *Microcavities* (Oxford University Press, Oxford, 2007).

[2] J. Kasprzak, M. Richard, S. Kundermann, A. Baas, P. Jeambrun, J. M. J. Keeling, F. M. Marchetti, M. H. Szymańska, R. André, J. L. Staehli, V. Savona, P. B. Littlewood, B. Deveaud, and L. S. Dang, Nature (London) **443**, 409 (2006).

[3] S. Christopoulos, G. B. H. von Högersthal, A. Grundy, P. G. Lagoudakis, A. V. Kavokin, J. J. Baumberg, G. Christmann, R. Butté, E. Feltin, J.-F. Carlin, and N. Grandjean, Phys. Rev. Lett. **98**, 126405 (2007).

[4] M. Saba, C. Ciuti, J. Bloch, V. Thierry-Mieg, R. André, L. S. Dang, S. Kundermann, A. Mura, G. Bongiovanni, J. L. Staehli, and B. Deveaud, Nature (London) **414**, 731 (2001).

[5] C. Weisbuch, M. Nishioka, A. Ishikawa, and Y. Arakawa, Phys. Rev. Lett. **69**, 3314 (1992).

[6] T. Yoshie, A. Scherer, J. Hendrickson, G. Khitrova, H. M. Gibbs, G. Rupper, C. Ell, O. B. Shchekin, and D. G. Deppe, Nature (London) **432**, 200 (2004).

[7] G. Oohata, T. Nishioka, D. Kim, H. Ishihara, and M. Nakayama, Phys. Rev. B **78**, 233304 (2008).

[8] D. G. Lidzey, D. D. C. Bradley, M. S. Skolnick, T. Virgili, S. Walker, and D. M. Whittaker, Nature (London) **395**, 53 (1998).

[9] D. G. Lidzey, D. D. C. Bradley, T. Virgili, A. Armitage, M. S. Skolnick, and S. Walker, Phys. Rev. Lett. **82**, 3316 (1999).

[10] M. Oda, K. Hirata, T. Inoue, Y. Obara, T. Fujimura, and T. Tani, Phys. Stat. Sol. (c) **6**, 288 (2009).

[11] K. Ishii, S. Nakanishi, and N. Tsurumachi, Appl. Phys. Lett. **103**, 013301 (2013).

[12] R. F. Oulton, N. Takada, J. Koe, P. N. Stavrinou, and D. D. C. Bradley, Semicond. Sci. Technol. **18**, S419 (2003).

[13] H. Kondo, Y. Yamamoto, A. Takeda, S. Yamamoto, and H. Kurisu, J. Lumin. **128**, 777 (2008).

[14] T. Schwartz, J. A. Hutchison, C. Genet, and T. W. Ebbesen, Phys. Rev. Lett. **106**, 196405 (2011).

[15] S. Gambino, M. Mazzeo, A. Genco, O. D. Stefano, S. Savasta, S. Patanè, D. Ballarini, F. Mangione, G. Lerario, D. Sanvitto, and G. Gigli, ACS Photonics **1**, 1042 (2014).

[16] M. Funahashi, J. Mater. Chem. C **2**, 7451 (2014).

[17] M. Funahashi, Polym. J. **41**, 459 (2009).

[18] T. Kato, M. Yoshio, T. Ichikawa, B. Soberats, H. Ohno, and M. Funahashi, Nat. Rev. Mater. **2**, 17001 (2017).

[19] M. O'Neill and S. M. Kelly, Adv. Mater. **23**, 566 (2011).

[20] T. Christ, B. Glüsen, A. Greiner, A. Keuner, R. Sander, V. Stümpflen, V. Tsukruk, and J. H. Wendorff, Adv. Mater. **9**, 48 (1997).

[21] F. Yuksel, M. Durmus, and V. Ahsen, Dyes. Pigments **90**, 191 (2011).

[22] T. Yasuda, H. Ooi, J. Morita, Y. Akama, K. Minoura, M. Funahashi, T. Shimomura, and T. Kato, Adv. Funct. Mater. **19**, 411 (2009).

[23] X.-Q. Li, X. Zhang, S. Ghosh, and F. Würthner, Chem. Eur. J. **14**, 8074 (2008).

[24] M. Funahashi and A. Sonoda, Org. Electron. **13**, 1633 (2012).

[25] M. Funahashi and A. Sonoda, J. Mater. Chem. **22**, 25190 (2012).

[26] Y. Hosokawa, M. Misaki, S. Yamamoto, M. Torii, K. Ishida, and Y. Ueda, Appl. Phys. Lett. **100**, 203305 (2012).

[27] J. Wenus, L. G. Connolly, D. M. Whittaker, M. S. Skolnick, and D. G. Lidzey, Appl. Phys. Lett. **85**, 5848 (2004).

[28] S. Hashimoto and M. Itoh, Jpn. J. Appl. Phys. **27**, 726 (1988).

[29] H. Kondo, A. Takeda, T. Tomikawa, H. Kurisu, S. Yamamoto, and M. Matsuura, J. Lumin. **119**, 137 (2006).

[30] Z. Chen, V. Stepanenko, V. Dehm, P. Prins, L. D. A. Siebbeles, J. Seibt, P. Marquetand, V. Engel, and F. Würthner, Chem. Eur. J. **13**, 436 (2007).

[31] J. R. Tischler, M. S. Bradley, Q. Zhang, T. Atay, A. Nurmikko, and V. Bulović, Org. Electron. **8**, 94 (2007).

[32] M. Fox, *Quantum Optics* (Oxford University Press, New York, 2006), Chap. 10, p. 208.

[33] P. A. Hobson, W. L. Barnes, D. G. Lidzey, G. A. Gehring, D. M. Whittaker, M. S. Skolnick, and S. Walker, Appl. Phys. Lett. **81**, 3519 (2002).

[34] S. Kéna-Cohen, S. A. Maier, and D. D. C. Bradley, Adv. Optical. Mater. **1**, 827 (2013).